Fluorescence Decay Characteristics of Indole Compounds Revealed by Time-Resolved Area-Normalized Emission Spectroscopy

Takuhiro Otosu, Etsuko Nishimoto, and Shoji Yamashita*

Institute of Biophysics, Faculty of Agriculture, Graduate School of Kyushu University, Hakozaki, Fukuoka 812-8581, Japan

Received: September 5, 2008; Revised Manuscript Received: November 13, 2008

Time-resolved fluorescence spectroscopy of tryptophan residue has been extensively applied to the studies on structure−function relationships of protein. Regardless of this, the fluorescence decay mechanism and kinetics of tryptophan residue in many proteins still remains unclear. Previous studies have demonstrated that conformational heterogeneity and relaxation dynamics are both involved in the peculiar multiexponential decay kinetics in subnanosecond resolution. In the present study, we characterized the fluorescence decay property of six indole compounds in glycerol by resolving the contribution of conformational heterogeneity and relaxation dynamics. We applied the time-resolved area-normalized fluorescence emission spectrum (TRANES) method for the fluorescence decay analysis. The results of TRANES, time-dependent shift of fluorescence spectral center of gravity, and fluorescence decay simulation demonstrated that the dielectric relaxation process independent of intrinsic rotamer/conformer and the individual fluorescence lifetime gives the peculiarity to the fluorescence decay of indole compounds. These results confirmed that TRANES and time-dependent spectral shift analysis are potent methods to resolve the origin of multiexponential decay kinetics of tryptophyl fluorescence in protein.

1. Introduction

The fluorescence of an aromatic amino acid, especially tryptophan residue, has been extensively applied to study structure−function relationships of proteins.[1−12] It is largely due to its sensitivity to subtle changes of conformation and local electric field surrounding tryptophan. Above all, time-resolved fluorescence spectroscopy has been widely used to study important biological systems such as protein−ligand interactions,[13] folding/unfolding mechanisms of proteins,[12,14] and channel formation.[2]

In principle, fluorescence from one fluorophore excited by an extremely short pulse decays exponentially. However, the fluorescence decays of some indole compounds and many single-tryptophan containing proteins such as melittin, subtilisin, and phospholipase A2 give the best fit only by multiexponential functions.[13,15] In order to obtain more interesting information about proteins through tryptophyl fluorescence, the origin and mechanism of the multiexponentiality of the tryptophyl fluorescence decay must be solved.

Hitherto, several kinetic models have been proposed to explain the multiexponential decay of tryptophan in subnanosecond resolution. Szabo and Rayner showed in their pioneering work that the fluorescence decay was described with a linear combination of exponentials with wavelength-independent decay time. Based on it, they have rationalized the peculiarity of the fluorescence decay of tryptophan in terms of different rotamers/conformers due to the rotation about a $C^{\alpha}-C^{\beta}$ bond of tryptophan.[16] NMR studies supported their model by verifying the existence of the population of rotamers coincident with the fluorescence results.[17,18] So the multiexponential decay of tryptophyl fluorescence in protein reported until now mostly interpreted with their rotamer/conformer model.[19−22]

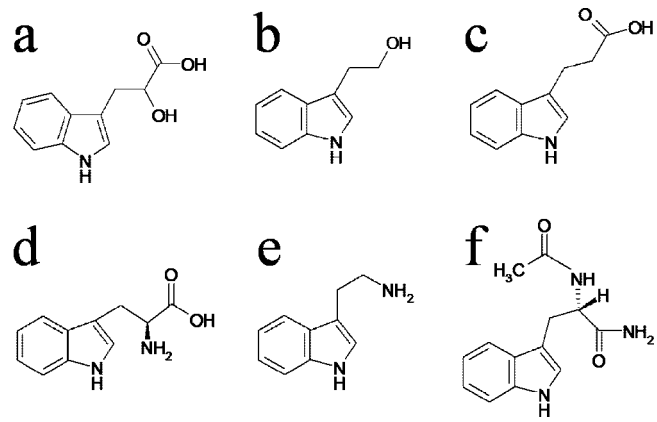

Figure 1. Chemical structures of 3-indolelactic acid (a), tryptophol (b), 3-indolepropionic acid (c), tryptophan (d), tryptamine (e), and *N*-acetyl-L-tryptophanamide (f).

Recently, Toptygin et al. proposed dielectric relaxation model[23] and applied it to the nanosecond relaxation dynamics study of single-tryptophan mutant of IIA^{Glc} protein[24] and B1 domain of Streptococcal protein G.[25] Their studies emphasized that the dielectric relaxation process around the indole of which dipole moment was enlarged in the excited singlet state exclusively influenced the fluorescence decay property in the protein matrix. Our time-resolved fluorescence study of melittin-calmodulin interaction also confirmed the involvement of dielectric relaxation process in fluorescence decay kinetics of tryptophan residue in protein complex.[13] Actually, the time-dependent red shift in the fluorescence of other solvatochromic dyes such as PRODAN has been examined in the studies of proteins,[26,27] membranes,[28] and DNA.[29] Furthermore, it is generally known that electrostatic interactions responsible for the fluorescence properties of intrinsic and extrinsic fluorophore play important role in a variety of biological process.[30,31]

* To whom correspondence should be addressed. E-mail: yamashita@brs.kyushu-u.ac.jp. Tel/Fax: +81-92-642-4425.

10.1021/jp8078937 CCC: $40.75
Published on Web 03/02/2009

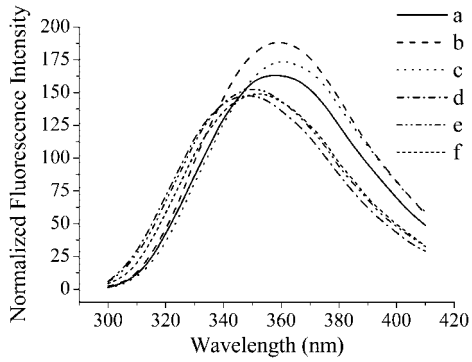

Figure 2. Steady-state fluorescence spectra of 3-indolelactic acid (a), tryptophol (b), 3-indolepropionic acid (c), tryptophan (d), tryptamine (e), and *N*-acetyl-L-tryptophanamide (f). The excitation wavelength was 285 nm. Excitation and emission band passes are 2 and 5 nm, respectively.

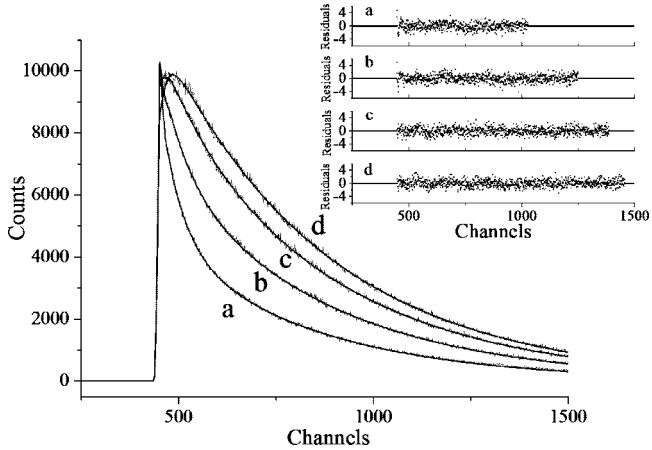

Figure 3. Fluorescence decay profiles and their residuals (inset) of tryptophol measured at 320 (a), 340 (b), 360 (c), and 380 (d) nm. The excitation wavelength was 285 nm. All experimental data was fitted with a sum of exponentials and these fitting lines are shown by solid lines.

Previous studies have approached the puzzle of "Why is there a nonexponential decay of single tryptophyl fluorescence in protein?" from the point of dielectric relaxation or conformational heterogeneity. However, at the same time, they have provided some evidence that both of them are involved in fluorescence decay of tryptophan, and those phenomena are also important aspects to study structure−function relationships of proteins. So far, there is no quantitative approach to resolve the contribution of the conformational heterogeneity and the dielectric relaxation process to the fluorescence decay of tryptophan into kinetics.

Indole compounds have a rotamer, and the conformational heterogeneities originated from it are known to affect the fluorescence decay in aqueous solution.[16] On the other hand, indole compounds in glycerol are expected by its intrinsic dipole moment and viscosity that the relaxation dynamics through the induced dipole−dipole interaction in the excited state occurs on a nanosecond scale. Therefore, the indole compounds in glycerol are excellent objects to clear the fluorescence decay mechanism including essential information about conformational heterogeneity and relaxation dynamics in the nanosecond region.

Toptygin et al. examined the effect of static heterogeneous ensemble on peak-normalized instantaneous fluorescence emission spectra usually abbreviated as TRES.[24] In the present study, we constructed time-resolved area-normalized emission spectra

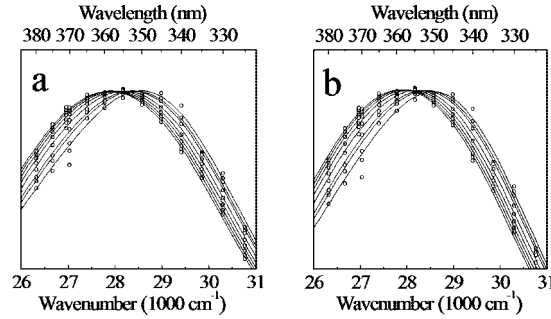

Figure 4. Time-resolved peak-normalized (a) and area-normalized (b) fluorescence spectra of tryptophol. Experimental data are shown by circles and those data are fitted by eq 6. Fitting lines are shown by solid lines. Times are 0.05, 0.08, 0.1, 0.15, 0.2, 0.25, 0.3, and 0.35 ns after excitation in order of decreasing wavenumber.

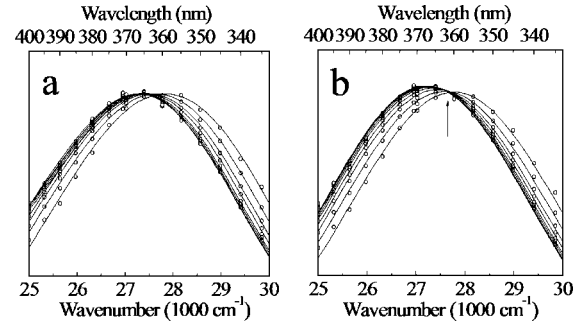

Figure 5. Time-resolved peak-normalized (a) and area-normalized (b) fluorescence spectra of tryptophol. Experimental data are shown by circles and those data are fitted by eq 6. Fitting lines are shown by solid lines. Times are 0.4, 0.8, 1.4, 2.0, 2.8, 3.6, 5, 6, and 8 ns after excitation in order of decreasing wavenumber. Arrow indicates the position of isoemissive point.

(TRANES) in addition to TRES. TRANES has been used to analyze two emitting species,[32−37] and if there is only one emitting species, the spectral shape of TRANES is same as that of TRES. This characteristic provides an important criterion to extract the dominant factor controlling the fluorescence decay of indole compounds.

In the present study, we examined fluorescence decay properties of six indole compounds in glycerol and resolved the involvement of the conformational heterogeneity and relaxation dynamics by TRANES.

2. Experimental Section

2.1. Sample Preparation. Tryptophan, *N*-acetyl-L-tryptophanamide (NATA), tryptamine, D,L-3-indole-lactic acid (lactic acid), and tryptophol were purchased from Sigma-Aldrich (St. Louis, MO), and 3-indolepropionic acid (propionic acid) was purchased from Wako (Osaka, Japan). They were commercially available and pure and so were used without further purification. Chemical structures of these six indole compounds are shown in Figure 1. Other reagents were of analytical grade and used without further purification. Sample preparation was according to the methods of Toptygin et al.[21] Briefly, a small aliquot of indole compounds in ethanol solution were added into glycerol for dilution. The concentrations of indole compounds were adjusted to give absorbance at 285 nm (A_{285}) < 0.1. These sample solutions were incubated in the dark at 20 °C for two days to complete the equilibrium.

2.2. Steady-State and Time-Resolved Fluorescence Measurements. Steady-state fluorescence measurements were performed on Hitachi 850 fluorescence spectrophotometer (Tokyo,

TABLE 1: Emission Wavelength Dependence of Fluorescence Decay Parameters

	λ (nm)	α_1	α_2	α_3	τ_1(ns)	τ_2(ns)	τ_3(ns)	τ_{ave}(ns)	sigma	SVR
lactic acid	320	0.34	0.32	0.34	6.20	1.02	0.22	5.35	1.01	1.85
	340	0.56	0.27	0.17	6.56	1.23	0.22	6.06	1.02	1.97
	360	0.87	0.17	−0.03	6.70	1.71	0.36	6.47	1.03	1.82
	380	1.26		−0.26	6.67		0.29	6.73	1.01	1.92
tryptophol	320	0.29	0.30	0.41	6.29	0.89	0.11	5.48	1.08	1.79
	340	0.48	0.24	0.29	6.69	1.05	0.07	6.24	1.07	1.76
	360	0.89	0.15	−0.04	6.85	1.67	0.32	6.66	1.05	1.86
	380	1.29		−0.29	6.80		0.32	6.87	1.01	1.85
propionic acid	320	0.29	0.31	0.39	6.34	0.86	0.13	5.52	1.04	1.95
	340	0.55	0.26	0.19	6.95	1.22	0.25	6.44	1.05	1.83
	360	0.85	0.15		7.02	1.64		6.81	1.03	1.96
	380	1.23		−0.23	7.10		0.30	7.15	1.06	1.81
tryptophan	320	0.46	0.32	0.22	4.98	0.95	0.16	4.45	1.00	2.03
	340	0.75	0.25		5.25	1.18		4.97	1.05	1.88
	360	1.02	0.23	−0.25	5.69	2.66	0.18	5.44	1.00	1.99
	380	1.34		−0.34	5.50		0.44	5.60	1.05	1.84
tryptamine	320	0.43	0.32	0.25	5.19	0.88	0.17	4.63	1.00	1.94
	340	0.66	0.24	0.11	5.53	1.14	0.12	5.21	1.09	1.75
	360	1.01	0.20	−0.20	5.90	3.12	0.17	5.66	1.04	2.01
	380	1.51	−0.14	−0.37	5.68	0.97	0.27	5.82	1.05	1.94
NATA	320	0.37	0.34	0.28	4.92	0.73	0.10	4.36	1.04	1.77
	340	0.56	0.25	0.18	5.35	0.97	0.08	5.00	1.09	1.71
	360	0.79	0.21		5.91	2.72		5.56	1.12	1.53
	380	1.29		−0.29	5.66		0.32	5.73	1.13	1.66

Japan). The excitation wavelength was set to 285 nm and band passes of excitation and emission were 2 and 5 nm, respectively. The fluorescence emission spectra were strictly corrected against the detection and excitation systems. Undesired effects of stray light were also removed by subtraction.

Time-resolved fluorescence measurements were performed with the subpicosecond laser based time-correlated single photon counting method (TCSPC) on an apparatus as described by Fukunaga et al.[14] The fluorescence decay property and the relaxation kinetics of indole compounds were almost the same irrespective of the excitation wavelength (data not shown). Therefore, the excitation wavelength was set to 285 nm. An excitation pulse was generated from a combination of subpicosecond Ti:sapphire laser (Tsunami, Spectra-Physics, MountainView, CA), pulse picker with second harmonic generator (model 3980, Spectra-Physics), and third harmonic generator (GWU, Spectra-Physics). The repetition rate was set at 800 kHz, and the excitation pulse width obtained was fwhm = 100 fs. The stop pulse to drive the time to amplitude converter (TAC, 457, Ortec, Oak Ridge, TN) was detected by a high speed APD (C5658, Hamamatsu Photonics, Shizuoka, Japan) followed by constant fraction discriminator (CFD, 935, Ortec). The fluorescence emission pulse was detected and amplified by a multichannel plate type photomultiplier (3809U-50, Hamamatsu Photonics), high speed amplifier (C5594, Hamamatsu Photonics), and fast timing amplifier (FTA820, Ortec). Those signals were fed into TAC through a CFD. The output signals of TAC were accumulated in 2048 channels in a multichannel analyzer (Maestro-32, Ortec). The channel width was 16.13 ps/ch. The full width at half-maximum (fwhm) of the instrument response function was 150 ps. The excitation pulse was vertically polarized, and emission signals were detected through a Glan-Taylor polarizer oriented 54.7° against the vertical.

2.3. Fluorescence Decay Analysis. The fluorescence decay kinetics were described with a linear combination of exponentials

$$F_\nu(\nu, t) = \sum_{i=1}^{N\exp} \alpha_i(\nu)\exp\{-t/\tau_i(\nu)\} \quad (1)$$

where $F_\nu(\nu,t)$ is the spectrally- and time-resolved fluorescence decay, $\tau_i(\nu)$ is the wavenumber-dependent fluorescence decay time of i-th component and $\alpha_i(\nu)$ is the corresponding pre-exponential factor. $\alpha_i(\nu)$ and $\tau_i(\nu)$ were determined by iterative convolution and nonlinear curve fitting methods. The average lifetime τ_{ave} was expressed as follows:

$$\tau_{ave} = \frac{\sum \alpha_i \tau_i^2}{\sum \alpha_i \tau_i} \quad (2)$$

The adequacy of curve-fitting was judged by the residual plots, the serial variance ratio (SVR), and the sigma value.[38]

The time-dependent shift of the fluorescence spectral center of gravity $\bar{\nu}(t)$ was expressed as follows:

$$\bar{\nu}(t) = \frac{\int_0^\infty \nu I(\nu, t)\, d\nu}{\int_0^\infty I(\nu, t)\, d\nu} \quad (3)$$

$$I(\nu, t) = \nu^{-3} F_\nu(\nu, t) \quad (4)$$

where $I(\nu,t)$ is the time-resolved fluorescence spectrum. It is denoted that preexponential factors in eq 1 were collected by multiplying $F_\nu^{SS}/\Sigma\alpha_i(\nu)\tau_i(\nu)$ where F_ν^{SS} is steady-state fluorescence intensity. The time-dependent shift of the center of gravity can be fitted with sum of exponentials and a constant described as follows:

$$\bar{\nu}(t) = \sum \alpha_{\nu i} \exp(-t/\tau_{\nu i}) + \nu(\infty) \quad (5)$$

where $\tau_{\nu i}$ is the relaxation time of the center of gravity of ith component, $\alpha_{\nu i}$ is the corresponding amplitude, and $\nu(\infty)$ is the relaxation limit of the center of gravity.

To construct TRANES from eq 3, we need to know the area value of each spectrum. Therefore, fluorescence decay data covering the entire spectral region is required, which is difficult

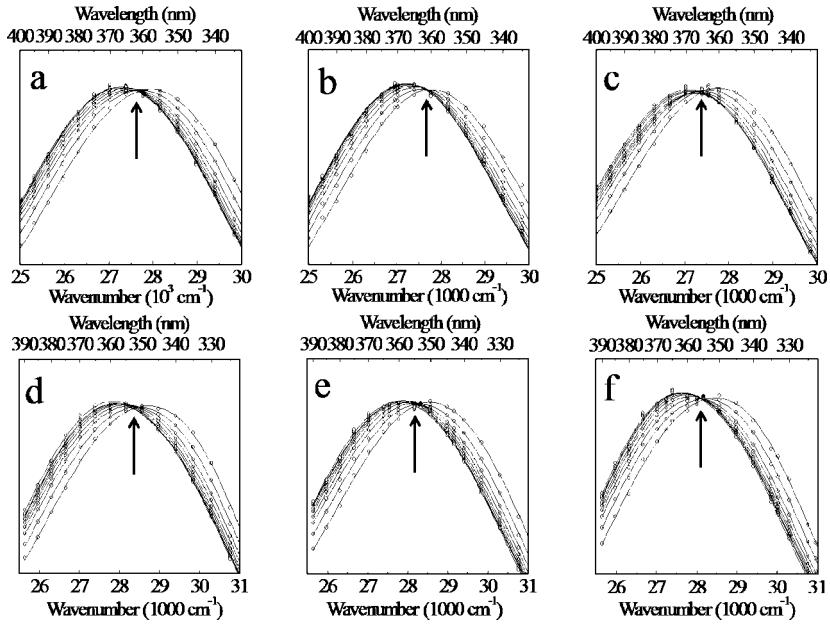

Figure 6. Time-resolved area-normalized fluorescence spectra of DL-3-indolelactic acid (a), tryptophol (b), 3-indolepropionic acid (c), tryptophan (d), tryptamine (e), and *N*-acetyl-L-tryptophanamide (f). Experimental data are shown by circles and those data are fitted by eq 6. Fitting lines are shown by solid lines. Times are 0.4, 0.8, 1.4, 2.0, 2.8, 3.6, 5, 6, and 8 ns after excitation in order of decreasing wavenumber. Arrows indicate the position of isoemissive point.

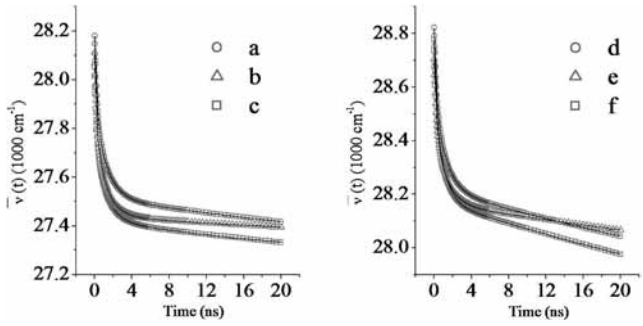

Figure 7. Time-dependent shifts of fluorescence spectral centers of gravity of D,L-3-indolelactic acid (a), tryptophol (b), and 3-indolepropionic acid (c) [left panel] and tryptophan (d), tryptamine (e), and *N*-acetyl-L-tryptophanamide (f) [right panel]. Experimental data are shown by symbols and those are fitted by eq 5. Fitting lines are shown by solid lines.

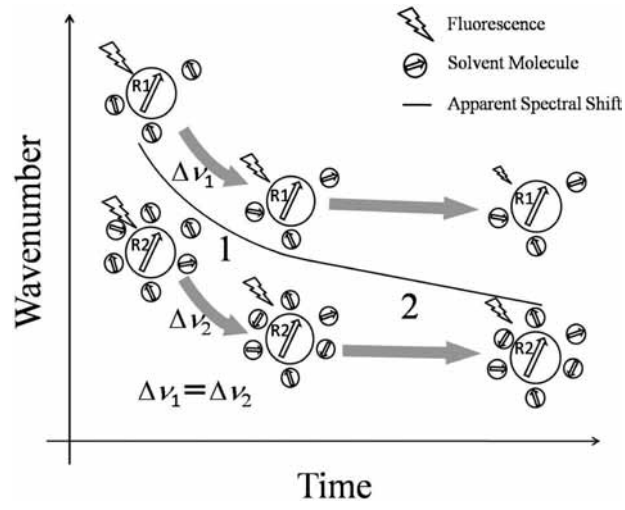

Figure 8. Fluorescence decay kinetics model of indole compounds including conformational heterogeneity and dielectric relaxation kinetics. R1 and R2 represent two rotamers/conformers. Solid black arrows show the directions of indole and solvent dipole moment. The intensities of fluorescence are expressed as the size of the objects. Numbers denoted in Figures 1 and 2 represent energy relaxation processes in subnanosecond and nanosecond time scale, respectively.

because of its weakness of signal at around the edge of the spectrum. In this study, we measured fluorescence decay of indole compounds at 305−400 nm at 5-nm intervals and fitted each time-resolved fluorescence spectrum with double Gaussian line shape equations expressed as follows to estimate the area of the spectra:

$$I(\nu, t) = \sum_{i=1}^{2} (A_i(t)/w_i(t)(\pi/2)^{1/2}) \exp(-2((\nu - \nu_i(t))/w_i)^2) \quad (6)$$

where $A_i(t)$ is the area, $w_i(t)$ is the full-width at half-maximum, and $\nu_i(t)$ is the center of gravity of each spectrum of ith component.

3. Results and Discussion

Figure 2 shows steady-state fluorescence spectra of lactic acid (a), tryptophol (b), propionic acid (c), tryptophan (d), tryptamine (e), and NATA (f). These indole compounds could be separated into two groups according to their emission maximum. Lactic acid, tryptophol, and propionic acid gave the emission peaks at around 360 nm (group 1). The other group included tryptophan, tryptamine, and NATA of which the emission peaks were found at around 350 nm (group 2). Quantum yields of the indole compounds of group 1 were higher than that of group 2.

Figure 3 shows fluorescence decay curves of tryptophol at some representative emission wavelengths. They showed the steep and truncated decay forms measured at the wavelength sides shorter and longer than the fluorescence emission maximum, respectively. Such features were also seen in the decay curves of other indole compounds. The fluorescence decay kinetics of six indole compounds were described with a linear combination of double or triple exponentials. Their decay parameters giving the best fit are summarized in Table 1. In

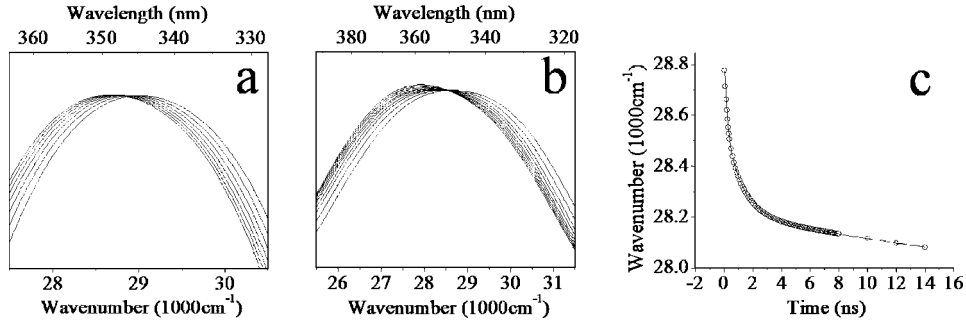

Figure 9. Time-resolved area-normalized fluorescence spectra (a, b) and time-dependent shift of the center of gravity (c) of simulated fluorescence decay kinetics model. Times are 0.05, 0.1, 0.15, 0.2, 0.25, 0.3, and 0.35 (a) and 0.4, 0.8, 1.4, 2, 3, 4, 6, 8, and 10 (b) ns. Calculated fluorescence spectral centers of gravity are shown by circles and those data are fitted by eq 5. Fitting lines are shown by solid lines (c).

TABLE 2: Fitting Parameters of Time-Dependent Shifts of Fluorescence Spectral Center of Gravities

	$\nu(0)$ (cm^{-1})	$\nu(\infty)$ (cm^{-1})	$\alpha_{\nu1}$ (cm^{-1})	$\alpha_{\nu2}$ (cm^{-1})	$\alpha_{\nu3}$ (cm^{-1})	$\tau_{\nu1}$ (ns)	$\tau_{\nu2}$ (ns)	$\tau_{\nu3}$ (ns)
lactic acid	28230	27192	330	380	330	0.22	1.25	53.56
tryptophol	28177	27330	360	370	110	0.17	1.14	34.72
propionic acid	28106	27219	320	360	210	0.19	1.12	33.39
tryptophan	28866	27408	270	370	810	0.2	1.16	80.32
tryptamine	28745	27537	270	310	630	0.23	1.21	113.2
NATA	28835	27242	260	400	940	0.14	0.95	82.60

TABLE 3: Dielectric Relaxation and Fluorescence Decay Parameters for Simulation

	$\nu(0)$ (cm^{-1})	$\nu(\infty)$ (cm^{-1})	w (cm^{-1})	$\alpha_{\nu1}$ (cm^{-1})	$\alpha_{\nu2}$ (cm^{-1})	$\tau_{\nu1}$ (ns)	$\tau_{\nu2}$ $\tau_{\nu2}$ (ns)	α	τ (ns)
R1	31010	30140	280	350	520	0.20	1.18	0.30	5.18
R2	28200	27330	380	350	520	0.20	1.18	0.70	5.75

TABLE 4: Emission Wavelength Dependence of Fluorescence Decay Parameters for Simulation

λ (nm)	α_1	α_2	α_3	τ_1 (ns)	τ_2 (ns)	τ_3 (ns)	τ_{ave} (ns)
320	0.64	0.23	0.14	5.31	0.98	0.21	5.01
340	0.94	0.05	0.01	5.49	1.21	0.26	5.44
360	1.09	−0.04	−0.05	5.68	0.72	0.16	5.71
380	1.43	−0.25	−0.19	5.74	0.94	0.19	5.91

every case, the average lifetime increased with increasing emission wavelength. One or two decay components with negative pre-exponential factor were recognized at the red side of the emission wavelength, and the corresponding lifetimes were almost coincident with the shorter lifetimes with positive pre-exponential factor at the blue side of the emission wavelength. Such wavelength dependence is substantial evidence indicating the close involvement of the dielectric relaxation process in the fluorescence decay of indole compounds in glycerol.

By using the experimentally decided parameters shown in Table 1, we constructed time-resolved peak-normalized (TRES) and area-normalized (TRANES) emission spectra. Figure 4 shows the resulting TRES and TRANES of tryptophol on a subnanosecond time scale. The maximum wavelengths observed in both types of time-resolved spectra gradually shifted to the red side with time, and the spectral line shape in TRANES was almost same as the one in TRES. Also in two time resolution procedures of the other five indole compounds, the time-evolving pattern of each spectrum in TRANES was coincident with that in TRES (data not shown). On the contrary, two types of time-resolved fluorescence spectra showed distinctive shapes in the nanosecond time range. TRES and TRANES of tryptophol in nanosecond region are shown in Figure 5. The beautiful isoemissive point was not found in TRES but in TRANES (Figure 5B). Figure 6 shows TRANES of all six indole compounds in nanosecond time-window. Other five indole compounds also showed the isoemissive point in TRANES similarly to tryptophol.

Time-dependent shift of fluorescence spectral center of gravity of six indole compounds are shown in Figure 7. The left and right panels in Figure 7 show the shifts of groups 1 and 2, respectively. It is noted that the dielectric relaxation process could not be described with single step. The emission centers of gravity of each indole compound steeply shifted in the range of 0−2 ns and then, moderately to reach the constant value. They were analyzed by a linear combination of exponentials using eq 5. Table 2 shows the resulting parameters for the time-dependent fluorescence spectral shift of the center of gravity of six indole compounds. They could be described with triple exponentials and a constant [$\nu(\infty)$]. The fast ($\tau_{\nu1}$) and intermediate ($\tau_{\nu2}$) relaxation times were same order as two shorter fluorescence lifetimes (τ_1, τ_2) which has positive amplitude at blue side and negative one at red side of the emission wavelength. Furthermore, the relaxation times observed here were almost consistent with that of indole in glycerol previously reported by Toptygin et al.[23] Probably, the existence of two relaxation time would be responsible for the characteristic relaxation dynamics of indole compounds under the condition given by surrounding dipoles of glycerol.

The longest relaxation time ($\tau_{\nu3}$) was in the range of several tens nanoseconds and was much longer than other two relaxation times ($\tau_{\nu1}$, $\tau_{\nu2}$). Petrich et al. indicated in the study of indole compounds in aqueous solution that two of three rotamers are closely involved in their fluorescence decay properties. One of three rotamer could not be distinguished from another one due to the similarity of fluorescence quenching efficiency and transition energy difference although tryptophan has three probable rotamers responsible for its fluorescence decay.[39] Therefore, it is reasonably anticipated that the component giving

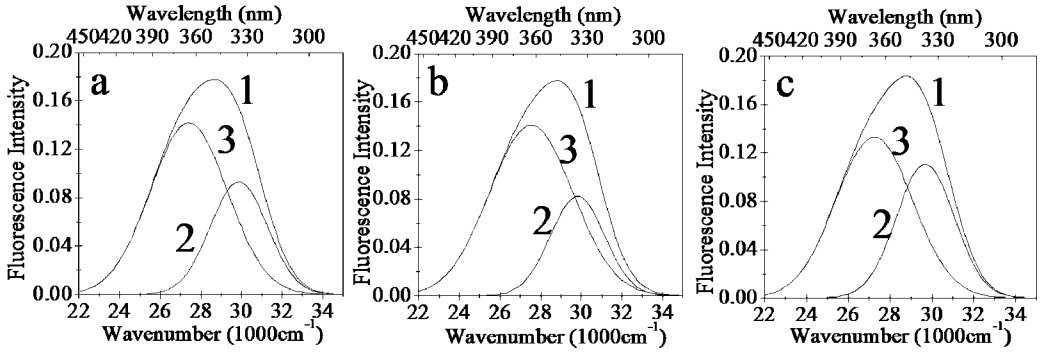

Figure 10. Constructed fluorescence spectra of tryptophan (a), tryptamine (b), and *N*-acetyl-L-tryptophanamide (c) after dielectric relaxation. Constructed fluorescence spectra of overall (1), R1 (2), and R2 (3) are shown by solid lines. Fluorescence spectra of R1 and R2 were constructed with Gaussian equation whose parameters were shown in Table 6, and that of the overall was constructed by summation of those spectra.

TABLE 5: Fitting Parameters of Time-Dependent Shifts of Fluorescence Spectral Center for Simulation

$\nu(0)$ (cm^{-1})	$\nu(\infty)$ (cm^{-1})	α_{v1} (cm^{-1})	α_{v2} (cm^{-1})	α_{v3} (cm^{-1})	τ_{v1} (ns)	τ_{v2} (ns)	τ_{v3} (ns)
28852	27404	269	373	806	0.27	1.16	80.32

TABLE 6: Calculated Fluorescence Centers of Gravity ($\nu(\infty)$, $\lambda(\infty)$), Full-Width at Half-Maximums (w) and Populations of Two Emitting Species (R1, R2) of Tryptophan, Tryptamine, and NATA after Dielectric Relaxation

		$\nu(\infty)$ (cm^{-1})	$\lambda(\infty)$ (nm)	w (cm^{-1})	distribution (%)
tryptophan	R1	29879	334.7	281	32.8
	R2	27408	364.9	379	67.2
tryptamine	R1	29824	335.3	267	27.5
	R2	27537	363.1	411	72.5
NATA	R1	29684	336.9	277	38.5
	R2	27242	367.1	369	61.5

the longest relaxation time would originate in the rotamer/conformer of indole compounds. In this context, the longest relaxation time and its amplitude originate depending on the population, fluorescence lifetime, and energy difference between relaxing excited-state and ground-state of two emitting species which consist of three rotamers.

Based on the above results, we propose a model for the fluorescence decay kinetics of indole compounds including conformational heterogeneity and dielectric relaxation (Figure 8). In subnanosecond time range, dielectric relaxation probably due to the reorientation of glycerol dipole following internal conversion from Franck−Condon state occurs. This process evolved independently on the primary solvation states of rotamers ($\Sigma\nu_1 = \Sigma\nu_2$). On the other hand, the ratio of fluorescence intensity between rotamers (R1 and R2) does not change because fluorescence lifetimes of each rotamers are much longer than subnanosecond (1). These characteristics bring the resemblance of TRANES and TRES in this time range. In the nanosecond time range in which the contribution of dielectric relaxation is much smaller, fluorescence decay characteristics of each rotamers determine the total fluorescence property (2). In this condition, TRANES shows isoemissive point and apparent fluorescence center of gravity shifts slowly with time toward the center of gravity of the rotamer which gives longer lifetime.

In order to confirm whether this model was valid or not, we attempted to construct TRANES and time-dependent shift of the center of gravity of fluorescence spectrum according to the model proposed here. Assigning the parameters about dielectric relaxation rates, fluorescence lifetimes, amplitudes and population of two rotamers (Table 3), the fluorescence decay as a function of emission wavelength, TRANES and time-dependent shift of fluorescence spectral center of gravity were simulated. The results are summarized in Tables 4 and 5. Constructed TRANES with different time scale and time-dependent shift of the center of gravity are shown in Figure 9. The characteristics of TRANES and time-dependent shift of the center of gravity were almost same as that of experimental data. Furthermore, the fitting parameters of time-dependent shift of fluorescence spectral center of gravity were perfectly in agreement with that of tryptophan (Tables 2 and 5). In this way, the decay characteristic of indole compound in glycerol could be reproduced by the model considering the involvement of two rotamers following dielectric relaxation process.

To characterize the rotamers of each indole compounds, we determined the fluorescence spectra at 5 ns after the excitation with the double Gaussian line shape function. Then, it was assumed that the total fluorescence emission was consisted of two rotamers, R1 and R2, which gave their maxima at higher and lower wavenumber side respectively, and that the value of center of gravity at infinitive time, $\nu(\infty)$ of each indole compounds was originated from R2. Table 6 shows the fluorescence spectral characteristics of two rotamers of each indole compounds in group 2 after completing the dielectric relaxation. The spectrum of group 1 could be described with single Gaussian line shape equation, because the energy distribution of R1 and R2 was extremely similar. Indeed, the value of longest relaxation time (τ_{v3}) and its amplitude (α_{v3}) of group 1 were smaller than that of group 2. The difference in the fluorescence spectral properties between rotamers of group 1 and group 2 might be originated from their solvation structure. Glycerol has three hydrophilic alcoholic hydroxyl groups. The substituents of group 1 also consist of hydroxyl and carboxyl groups. The same and/or resembled substituent might give the indole compounds of group 1 homogeneous electric field to allow the more efficient relaxation of excited state. The proton donating properties of amino group would create the heterogeneous solvation structure in the group 2.

The populations of two rotamer responsible for the fluorescence decay of group 2 were calculated by using the parameters shown in Table 6 and the center of gravity of overall spectrum at 0 ns, that is, $\nu(\infty) + \alpha_{v3}$. The reconstructed fluorescence spectral profiles of each rotamer and overall emission after dielectric relaxation are shown in Figure 10. The R1 fraction of tryptophan was 32.8% and that of R2 was 67.2% (Table 6).

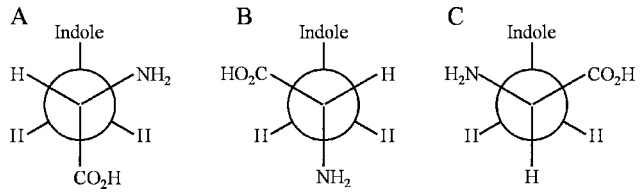

Figure 11. Three conformers of tryptophan about the $C^{\alpha}-C^{\beta}$ tryptophyl bond.

Our data suggested that R1 is attributed to the rotamers A and C in which the amino group is close to the indole moiety, and R2 would be attributed to rotamer B denoted in Figure 11. This assignment was consistent with the data proposed by Petrich et al.[39] although the population ratio of rotamers was slightly incompatible, and the ratio obtained by our data was also inconsistent with the one obtained by NMR.[17] These discrepancies might be due to solvent condition, and the fraction of rotamers proposed here is not one in the ground-state but the fluorescence fraction which depends on optical parameters and quantum yields of each rotamer.

In this study, any trace indicating conformational exchange between rotamers was not observed. Conformer interconversion rates of tryptophan and tyrosine about nanosecond lifetime were reported previously.[40,41] The reason why such interconversion was not observed is that glycerol would make the interconversion rate much slower than the value previously reported.

4. Conclusions

The TRANES method was applied to six indole compounds in glycerol to analyze the contribution of conformational heterogeneity and relaxation dynamics to fluorescence decay process. The TRANES of six indole compounds and their resulting time-dependent shift of fluorescence spectral center of gravity demonstrated that the most essential features characterizing the fluorescence process of indole compounds were the dielectric relaxation process independent of intrinsic rotamer/conformer and the individual fluorescence lifetime. The fluorescence decay simulation revealed that the model proposed here is reasonable.

Rationalizing the fluorescence decay property of tryptophan residue in protein is required to make physical image for the subtle conformation change of protein clearer by a time-resolved fluorescence method. If TRANES is applied to studies on the complex protein, their structure, function, and dynamics would be elucidated through the fluorescence property of tryptophan in protein.

References and Notes

(1) Oishi, O.; Yamashita, S.; Nishimoto, E; Lee, S.; Sugihara, G.; Ohno, M. *Biochemistry* **1997**, *36*, 4352.
(2) Lee, S.; Kiyota, T.; Kunitake, T.; Matsumoto, E.; Yamashita, S.; Anzai, K.; Sugihara, G. *Biochemistry* **1997**, *36*, 3782.
(3) Nishimoto, E.; Yamashita, S.; Szabo, A. G.; Imoto, T. *Biochemistry* **1998**, *37*, 5599.
(4) Nishimoto, E.; Yamashita, S.; Yamasaki, N.; Imoto, T. *Biosci. Biotechnol. Biochem.* **1999**, *63*, 329.
(5) Shaw, A. K.; Pal, S. K. *J. Photochem. Photobiol. B* **2008**, *90*, 69.
(6) Lakshmikanth, G. S.; Krishnamoorthy, G. *Biophys. J.* **1999**, *77*, 1100.
(7) Sardar, P. S.; Maity, S. S.; Ghosh, S.; Chatterjee, J.; Maiti, T. K.; Dasgupta, S. *J. Phys. Chem. B* **2006**, *110*, 21349.
(8) Stella, L.; Caccuri, A. M.; Rosato, N.; Nicotra, M.; Lo Bello, M.; De Matteis, F.; Mazzetti, A. P.; Federici, G.; Ricci, G. *J. Biol. Chem.* **1998**, *273*, 23267.
(9) Mei, G.; Di Venere, A.; De Matteis, F.; Rosato, N. *Arch. Biochem. Biophys.* **2003**, *417*, 159.
(10) Larsen, O. F. A.; van Stokkum, I. H. M.; Pandit, A.; van Grondelle, R.; van Amerongen, H. *J. Phys. Chem B* **2003**, *107*, 3080.
(11) Raghuraman, H.; Chattopadhyay, A. *Eur. Biophys. J.* **2004**, *33*, 611.
(12) Neyroz, P.; Zambelli, B.; Ciurli, S. *Biochemistry* **2006**, *45*, 8918.
(13) Otosu, T.; Nishimoto, E.; Yamashita, S. *J. Biochem.* **2007**, *142*, 655.
(14) Fukunaga, Y.; Nishimoto, E.; Yamashita, K.; Otosu, T.; Yamashita, S. *J. Biochem.* **2007**, *141*, 9.
(15) Lakowicz, J. R. *Principles of Fluorescence Spectroscopy*; Kluwer/Academic Plenum: New York, 1997.
(16) Szabo, A. G.; Rayner, D. M. *J. Am. Chem. Soc.* **1980**, *102*, 554.
(17) Skrabal, P.; Rizzo, V.; Baici, A.; Bangerter, F.; Luisi, P. L. *Biopolymers* **1979**, *18*, 995.
(18) Pan, C-P.; Barkley, M. D. *Biophys. J.* **2004**, *86*, 3828.
(19) Fernandez, R. M; Vieira, R. F.; Nakaie, C. R.; Lamy, M. T.; Ito, A. S. *Biopolymers* **2005**, *80*, 643.
(20) Marquezin, C. A.; Hirata, I. Y.; Juliano, L.; Ito, A. S. *Biopolymers* **2003**, *71*, 569.
(21) Harvey, B. J.; Bell, E.; Brancaleon, L. *J. Phys. Chem. B* **2007**, *111*, 2610.
(22) Hellings, M.; Maeyer, M. D.; Verheyden, S.; Hao, Q.; Damme, E. J. M. V.; Peumans, W. J.; Engelborghs, Y *Biophys. J.* **2003**, *85*, 1894.
(23) Toptygin, D.; Brand, L. *Chem. Phys. Lett.* **2000**, *322*, 496.
(24) Toptygin, D.; Savtchenko, R. S.; Meadow, N. D.; Brand, L. *J. Phys. Chem. B* **2001**, *105*, 2043.
(25) Toptygin, D.; Gronenborn, A. M.; Brand, L. *J. Phys. Chem. B* **2006**, *110*, 26292.
(26) Abbyad, P.; Shi, X.; Childs, W.; McAnaney, T. B.; Cohen, B. E.; Boxer, S. G. *J. Phys. Chem. B* **2007**, *111*, 8269.
(27) Guha, S.; Sahu, K.; Roy, D.; Mondal, S. K.; Roy, S.; Bhattachayya, K. *Biochemistry* **2005**, *44*, 8940.
(28) Hutterer, R.; Schneider, F. W.; Lanig, H.; Hof, M. *Biochem. Biophys. Acta* **1997**, *1323*, 195.
(29) Somoza, M. M.; Andreatta, D.; Murphy, C. J.; Coleman, R. S; Berg, M. A. *Nucleic Acids Res.* **2004**, *32*, 2494.
(30) Andersen, O. S.; Greathouse, D. V.; Providence, L. L.; Becker, M. D.; Koeppe, R. E. *J. Am. Chem. Soc.* **1998**, *120*, 5142.
(31) Hilvert, D. *Annu. Rev. Biochem.* **2000**, *69*, 751.
(32) Novaira, M.; Biasutti, M. A.; Silber, J. J.; Correa, N. M. *J. Phys. Chem. B* **2007**, *111*, 748.
(33) Koti, A. S. R.; Krishna, M. G.; Periasamy, N. *J. Phys. Chem. A* **2001**, *105*, 1767.
(34) Chorvat Jr, D.; Chorvatova, A. *Eur. Biophys. J.* **2006**, *36*, 73.
(35) Shaw, A. K.; Pal, S. K. *J. Phys. Chem. B* **2007**, *111*, 4189.
(36) Ira; Koti, A. S. R.; Krishnamoorthy, G.; Periasamy, N. *J. Fluoresc.* **2003**, *13*, 95.
(37) Koti, A. S. R.; Periasamy, N. *J. Chem. Phys.* **2001**, *115*, 7094.
(38) McKinnon, A. E.; Szabo, A. G.; Miller, D. R. *J. Phys. Chem.* **1977**, *81*, 1564.
(39) Petrich, J. W.; Chang, M. C.; McDonald, D. B.; Fleming, G. R. *J. Am. Chem. Soc.* **1983**, *105*, 3824.
(40) McMahon, L. P.; Yu, H-T.; Vela, M. A.; Morales, G. A.; Shui, L.; Fronczek, F. R.; McLaughlin, M. L.; Barkley, M. D. *J. Phys. Chem. B* **1997**, *101*, 3269.
(41) Unruh, J. R.; Liyanage, M. R.; Johnson, C. K. *J. Phys. Chem. B* **2007**, *111*, 5494.

JP8078937